JOURNAL OF AGRICULTURAL AND FOOD CHEMISTRY

Some Structural and Electronic Features of the Interaction of Phosphate with Metal−Humic Complexes

IÑAKI GUARDADO,[†] OSCAR URRUTIA,[‡] AND JOSE M. GARCIA-MINA*[,†,‡]

Department of Chemistry and Soil Chemistry, University of Navarra, 31080 Pamplona, Spain, and R&D Department, Inabonos-Roullier Group, Poligono Arazuri-Orcoyen, 31160 Orcoyen, Spain

Previous studies demonstrated the formation of stable phosphate−metal−humic complexes in solution. These studies, however, indicated that the proportion of complexed metal that intervenes in phosphate fixation is rather low. In this study we investigate the possible structural and electronic features of the binding site involved in phosphate fixation in metal−humic complexes that could explain this fact. To this end, we have studied phosphate−metal−humic complexes involving Fe(III), Al(III), and Zn(II) using three complementary techniques: infrared spectroscopy (FTIR), fluorescence, and molecular modeling. The FTIR study indicated that, in the case of those complexes involving Fe and Zn phosphate, fixation is associated with a stabilization of the metal−carboxylate bond. In the case of Al this effect is less clear. This effect of phosphate fixation on the characteristics of the metal−humic binding site was also supported by the results obtained in the Fluorescence study, which showed significant changes in the quenching effect normally associated with metal complexation in humic substances upon phosphate fixation. Finally, the molecular modeling study revealed that the stability of phosphate−metal−humic complexes is inversely related to the stability of the metal−humic interaction. This result could explain why only a relatively low proportion of humic complexed metal is involved in phosphate fixation.

KEYWORDS: Phosphate−metal−humic complexes; FTIR; fluorescence; molecular modeling; humic substances; salicylic binding model

INTRODUCTION

Numerous studies have reported the beneficial effect of organic matter on the potential bioavailability of phosphorus (P) for plants and microorganisms (*1*). In principle, these effects seem to involve different and complementary mechanisms. Among those related to P, solubility in soil solution seems to play an important role the formation of stable and soluble complexes between phosphate and humic substances (*2, 3*). In fact, a number of studies have demonstrated that stable organic complexes comprising humic substances and phosphate can indeed be formed via metal bridges (*4*–*6*). Guardado et al. (*6*) reported the formation of this type of complex in solution involving many different metals, both divalent (Zn, Cu, Mn, Ca, and Mg) and trivalent (Fe and Al). These complexes presented apparent stability constant values for the phosphate−metal−humic interaction in the same order of magnitude as the corresponding metal−humic complexes (*6*). This fact suggested that they could have an important influence on the fraction of available P is soils. However, this study confirmed previously reported results indicating that the fraction of the complexed metal that is involved in the fixation of phosphate is rather low (between 10 and 20% of the total complexed metal depending on the metal) (*4, 6*). In these studies, it was proposed that this might be the consequence of the significant molecular aggregation associated with metal complexation in humic systems (*6*). The results obtained, however, did not support this hypothesis, indicating that this fact must be associated in some way with one or several constraints linked to the electronic and/or steric features of the binding site (*6*).

To study those structural and/or electronic conditions that could govern the phosphate−metal−humic interaction, we investigate phosphate binding in specific metal−humic complexes using two complementary experimental techniques: infrared spectroscopy (FTIR) and fluorescence. We also complete the study by carrying out a theoretical study using molecular modeling methods (principally, molecular mechanics and semiempirical quantum chemical methods). To compare the influence of divalent and trivalent metals, we have considered humic−metal−phosphate complexes involving Al(III), Fe(III), and Zn(II).

Other instrumental techniques were also regarded to study the interaction of phosphate with metal−humic complexes. Among them, ^{31}P NMR spectroscopy was explicitly considered.

* Author to whom correspondence should be addressed. Telephone: (34)948324550; fax (34)948324032; e-mail: jgmina@inabonos.com.
[†] University of Navarra.
[‡] Poligono Arazuri-Orcoyen.

10.1021/jf072641k CCC: $40.75
Published on Web 01/19/2008

However, the relatively low concentration of fixed P in the complexes resulted in spectra with very poor resolution and reproducibility.

MATERIALS AND METHODS

Preparation of Humic Acid and Metal−Humic and Phosphate−Metal−Humic Complexes. The humic acid (HA) employed in the different experiments was one extracted from a leonardite obtained from the Czech Republic. The HA sample was first purified using the International Humic Substances Society (IHSS) methodology without including the HF-HCl mixture treatment. In short, 10 g of nondried leonardite were weighed in a 250 mL flask, to which 0.1 M NaOH was added until all of the air had been displaced. After 48 h of stirring at 25 °C in darkness, the supernatant containing the unfractionated humic extract was separated from the solid fraction by centrifugation at 7650*g* for 30 min. The HA was obtained by acidifying an aliquot of the alkaline extract containing the humic and fulvic acids obtained from leonardite with 6 M HCl up to a pH of 1.5. After 12 h, the acidified sample was centrifuged at 7650*g* for 30 min to separate the precipitated humic acid from the supernatant containing the fulvic acids and other acid-soluble organic compounds. After washing humic acids with water to eliminate Cl^- contamination, they were freeze-dried. The main composition of the purified HA was 58.47% C, 1.46% N, 2.69% H, 25.76% O, 0.01% P, 0.99% S, 1.02% Fe, and 0.95% Al. The contents of C, H, and N in HA were obtained using elemental analysis (LECO CHN 2000), whereas the contents of P, S, Fe, and Al were obtained by ICP-OES spectrometry (Thermo Elemental Co. Iris Intrepid II XDL). The content of O was calculated by difference. The main acidic functional group concentration, obtained using potentiometric analysis, was 1.98 mmol g^{-1} HA of carboxylic groups and 1.18 mmol g^{-1} HA of phenolic groups (*7*).

Metal−humic (M−HA) complexes were prepared as described in refs *4 and 6*. Briefly, to reach a 1.8 mmol metal/g C ratio, Fe(III), Al(III), and Zn(II) nitrate salts were dissolved in water and slowly dropped into 200 mL of the supernatant containing HA, under vigorous stirring and continuous pH control (*8, 9*) with NaOH. The solution was diluted to 500 mL, stirred for 14 h, and then centrifuged for 15 min at 7000*g* to separate M−HA complexes in solution from precipitated M−HA complexes and metal hydroxides. The phosphate−metal−humic complexes (PO_4^{3-}−M−HA) were prepared using a synthesis pathway involving two steps: step one consists of the formation of stable M−HA complexes at pH 8–9, and step two consists of the reaction of PO_4^{3-} with the M−HA complex at different pH values. This method has been used in previous studies (*4*). It involves the addition of 0.5 mM H_3PO_4 aliquots containing the necessary quantity of PO_4^{3-} to achieve specific metal/P molar ratios to each M−HA complex. The pH was kept at the final values 4, 6, or 8 with 0.5 M HNO_3 or 0.5 M NaOH, and ionic strength values stayed in the 0.01–0.02 M interval. Solutions were subsequently diluted up to 50 mL with pure water and were stirred for 14 h at 22 °C. Once the reactions were completed, the solutions were centrifuged for 15 min at 7000*g*. Finally, the total C, P, and metal content in solution were analyzed. To eliminate free P, the different complexes were purified using the HCO_3^- Anion Exchange Resin methodology described in ref *4*.

Elemental Analysis. The concentration of P (as PO_4^{3-}) in solution was analyzed using ICP-OES spectrometry (Thermo Elemental Co. Iris Intrepid II XDL). The C content in solution was analyzed using elemental analysis (LECO CHN 2000 and Shimadzu TOC-5050), and the metal content in solution was determined using ICP-OES spectrometry.

FTIR Spectroscopy. Pellets were prepared by mixing 0.5 mg of each freeze-dried sample corresponding to HA and to each M−HA complex and PO_4^{3-}−M−HA complex obtained at the different pH values used in the study (*4, 6, 8*), with 200 mg of KBr. Infrared spectra were recorded on these pellets with a Nicolet Magna-IR 550 Spectrometer over the 4000–400 cm^{-1} range.

Fluorescence. Solutions of each freeze-dried sample corresponding to HA and to each M−HA complex and PO_4^{3-}−M−HA complex obtained at the different pH values used in the study (*4, 6, 8*) were prepared by diluting the samples to 10 mg/L of total organic carbon. Synchronous Fluorescence spectra were recorded with a SFM-25 Fluorimeter (Kontron) over the 250–600 nm range at $\Delta\lambda = 18$ nm.

Molecular Modeling. A theoretical study of the chemical interaction between the different elements of the molecular system (HA, metals, and phosphate) was carried out using both molecular mechanics and semiempirical quantum mechanics methods. The operational and theoretical approaches were made assuming that intermolecular chemical interactions generally have two main, successive steps:

Step 1. A spatial convergence of the interacting molecules that is governed by electrostatic forces related to the electric charge distribution (atomic charges) on each molecule (the intermolecular convergence interaction is of an electrostatic nature) is assumed. This first step, which is the electrostatic interaction, was studied through the energy minimization of the molecular system using molecular mechanics. Both MM+ (*8*) and Amber (*9*) force fields were used, and the geometry and the atomic charges of the individual molecules were previously obtained using the semiempirical quantum mechanics method PM3 (*10*).

Step 2. A chemical interaction between specific regions of the molecules that have achieved the bond distance as a consequence of the electrostatic interaction (Step 1) is assumed. This step, which involves the creation of new chemical bonds, is the binding interaction. To study the binding interaction, we carried out the energy minimization of the chemical system obtained from the electrostatic interaction, using the semiempirical quantum chemical method PM3.

The model selected to represent binding sites in HA was a salicylic acid moiety. This selection was based on the following main reasons: (1) the results obtained in this study concerning fluorescence modification upon metal and phosphate complexation in HA binding sites indicate that these binding sites must be attached to fluorophores. These fluorophores are, probably, related to the aromatic moiety of the HA molecules (*11*). Among the possible chelating sites with aromatic character in HA, experimental evidence suggests the presence of ftalic, salicylic, and catechol groups (*11*). On the other hand, the variation pattern of the stability and the maximum binding ability for the interaction of different metals with HS extracted from different origin observed in previous studies indicated the involvement of both carboxylic and phenolic groups in the complexation process (*11, 12*). In consequence, a suitable model for this binding pattern is the salicylic group. It becomes clear, however, that this option involves a simplification of the process to make the study feasible. For this same reason, we have focused our interest in the binding site, without an explicit consideration of the structural environment and its influence on the electronic properties of the binding site. Likewise, the use of a specific binding site, separate of the structural environment (the whole macromolecule), implies the use of only one metal, because of the repulsion forces among positively charged metals.

The influence of pH is included in the model through the explicit consideration of two ionization patterns: the ionization of the carboxylic group only, and the ionization of both the carboxylic and phenol groups. The study was carried out on the systems involving Al(III) and Zn(II) because these two cations are well parametrized in the PM3 semiempirical method. The metals were modeled as Zn(II) and Al(III) in their pentahydrated and hexahydrated forms, respectively, because they are their main molecular forms in the pH interval considered in the study (*13*). Two main ionized forms for phosphate are present in the pH range of the study: $H_2PO_4^-$ and HPO_4^{-2} (*13*). We present here the results obtained using HPO_4^{-2} to model the phosphate anion. The results using $H_2PO_4^-$ were qualitatively similar to those corresponding to HPO_4^{-2}.

The study was developed following two steps: first, we considered the formation of the M−HA complex; second, we considered the interaction of PO_4^{3-} with the M−HA complex.

The relative stability of the interactions was assumed to be directly related to the value of the binding energy (E) calculated for the molecular interaction. The binding energy corresponding to the molecular interaction (ΔE_R) is calculated by the subtraction of the sum of the binding energy of the individual molecules involved in the interaction from the binding energy corresponding to the new molecule formed as a result of the interaction.

We do not compare our results with previous studies because these studies involved the assumption of a specific chelation mode, whereas

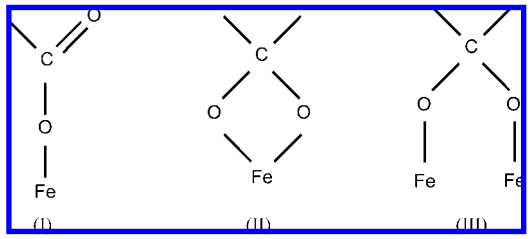

Figure 1. Examples of different modes of coordination for the interaction of Fe−carboxylate: (I) unidentate; (II) bidentate, and (III) bidentate-bridging.

in this study we explore the possible nature of the chelation mode. For all calculations carried out using PM3, a vibrational analysis was performed on all obtained structures to ensure the absence of negative vibrational frequencies and thus verify the existence of a true minimum. The study was carried out using the Hyperchem 7.0 software package.

RESULTS AND DISCUSSION

The FTIR Study. The FTIR spectra of the freeze-dried samples corresponding to both M−HA and PO_4^{3-}−M−HA complexes can provide some information about the microstructure of the binding sites associated with each interaction. From the point of view of interpreting the spectra, the most interesting zone is between 1000 and 1800 cm^{-1}. In this region the bands due to the asymmetric (ν_{asym}) and symmetric (ν_{sym}) stretches of the carboxylate group in HA appear, at 1624–1633 cm^{-1} and 1385–1383 cm^{-1}, respectively, depending on pH. A number of studies have demonstrated that when carboxylic acids and their salts form complexes with metals, frequency shifting and changes in the shape of the stretching bands of COO^- group occur (*14*). From the frequency shift, $\Delta\nu = \nu_{asym} - \nu_{sym}$, it is possible to identify the mode of coordination between the carboxylate and the metal by comparison to the salt (the potassium humate in our case). Thus, a unidentate structure (I) has distinct double C═O and single C−O bonds, whereas bidentate structures (chelating (II) or bidentate bridging (III)), will have equivalent C−O bonds (**Figure 1**). In the case of a unidentate structure, the ν_{asym} must appear at ca. 1620–1650 cm^{-1}, indicative of a C═O character, (with $\Delta\nu$ being higher than that of the corresponding monovalent salt), whereas the absence of such a characteristic band along with a $\Delta\nu$ lower that the corresponding salt implies a bidentate coordination (*14, 15*). In addition, if $\Delta\nu$ is similar to that of the salt, the resulting structure corresponds to bidentate-bridging.

In our study we have compared the $\Delta\nu$ values corresponding to each M−HA complex with that of HA, at each pH value, and the $\Delta\nu$ values corresponding to each PO_4^{3-}−M−HA to that of the corresponding M−HA complex, at each pH value. The comparisons are carried out at each pH value because the $\Delta\nu$ value corresponding to the potassium humate varies as a function of pH value. This effect is probably due to the influence of pH on the ionization degree of the carboxylate. The results describing $\Delta\nu$ variations are presented in **Table 1**.

Regarding Al−HA complexes, the results indicate that the process of metal complexation generates unidentate (pH 6) and bidentate-bridging (pH 4 and 8) interactions with the carboxylate. The process of fixation of PO_4^{3-} did not induce remarkable changes in the complexation mode.

In the case of Fe−HA complexes, the mode of metal complexation was similar to that of Al−HA complexes for pH 8. At pH 6, however, the complexation mode was bidentate-bridging, and at pH 4 it was bidentate. In this case, however, PO_4^{3-} fixation induced a clear reduction in $\Delta\nu$ for all pH values,

Table 1. Asymmetric and Symmetric Band of Carboxylate, Δ(asym−sym), and Binding Mode (Bidentate-Bridging, BD-BG; Bidentate, BD, and Unidentate, UD) for HA, M−HA Complexes and PO_4^{3-}−M−HA Complexes as a Function of pH

compound	asymmetric band	symmetric band	Δ (asym–sym)	binding mode
HA, pH 4	1624	1385	239	
HA, pH 6	1593	1385	208	
HA, pH 8	1581	1385	196	
Al−HA, pH 4	1628	1385	243	BD-BG
Al−HA, pH 6	1624	1385	239	UD
Al−HA, pH 8	1585	1385	200	BD-BG
PO_4^{3-}−Al−HA, pH 4	1628	1385	243	BD-BG
PO_4^{3-}−Al−HA, pH 6	1618	1385	233	UD
PO_4^{3-}−Al−HA, pH 8	1589	1385	204	BD-BG
Fe−HA, pH 4	1618	1385	233	BD
Fe−HA, pH 6	1595	1385	210	BD-BG
Fe−HA, pH 8	1589	1385	204	BD-BG
PO_4^{3-}−Fe−HA, pH 4	1583	1385	198	BD
PO_4^{3-}−Fe−HA, pH 6	1593	1400	193	BD
PO_4^{3-}−Fe−HA, pH 8	1583	1400	183	BD
Zn−HA, pH 4	1626	1385	241	BD-BG
Zn−HA, pH 6	1624	1385	239	UD
Zn−HA, pH 8	1592	1385	207	BD-BG/UD
PO_4^{3-}−Zn−HA, pH 4	1581	1385	196	BD
PO_4^{3-}−Zn−HA, pH 6	1583	1398	185	BD
PO_4^{3-}−Zn−HA, pH 8	1581	1385	196	BD-BG

which indicate a stabilization of a bidentate mode. Similar results were obtained for Zn complexes, because the clear unidentate (pH 6)/bidentate bridging (pH 4 and 8) modes associated with Zn complexation are transformed into a clear bidentate mode upon PO_4^{3-} fixation, except in the case of pH 8 (bidentate-bridging). These results indicate that in the case of Fe and Zn complexes the fixation of PO_4^{3-} in M−HA binding sites seems to induce significant changes in the electronic configuration of the binding site, leading to a stabilization of intramolecular M−HA bonds. These changes could be related to the molecular disaggregation associated with PO_4^{3-} fixation (*6*). In the case of Al complexes, however, this effect is less clear.

The Fluorescence Study. A number of studies have demonstrated that the process of metal complexation in organic ligands attached to fluorescent groups (such as aromatic rings) caused important changes in the fluorescence emission spectra, which are principally reflected in a quenching effect of the intensity of fluorescence (*16*). In the case of humic substances this effect has been used to analyze both the electronic characteristics and the stability of the binding process (*16*).

In the case of PO_4^{3-}−Al−HA complexes, PO_4^{3-} fixation induced different patterns of quenching depending on pH (**Figure 2**). Thus, at pH 4, PO_4^{3-} fixation was associated with a decrease in the intensity of the quenching effect linked to Al complexation in HA. This effect diminished at pH 6, whereas at pH 8 it represents an increase in the quenching.

Similar results were observed for PO_4^{3-}− Zn−HA complexes (**Figure 4**). In the case of PO_4^{3-}−Fe−HA complexes, however, PO_4^{3-} fixation was associated with a significant increase in the quenching effect at all pH values studied (**Figure 3**).

In principle, these results indicate that PO_4^{3-} fixation affects the electronic and structural features of the M−HA binding site. These results could be linked to changes in the stability of the M−HA interaction. Thus, PO_4^{3-} fixation might induce a possible debilitation at acidic pH and reinforcement at alkaline pH for Al and Zn complexes and a clear reinforcement for Fe complexes at both acidic and basic pH values. Thus, for Al and Zn at acidic

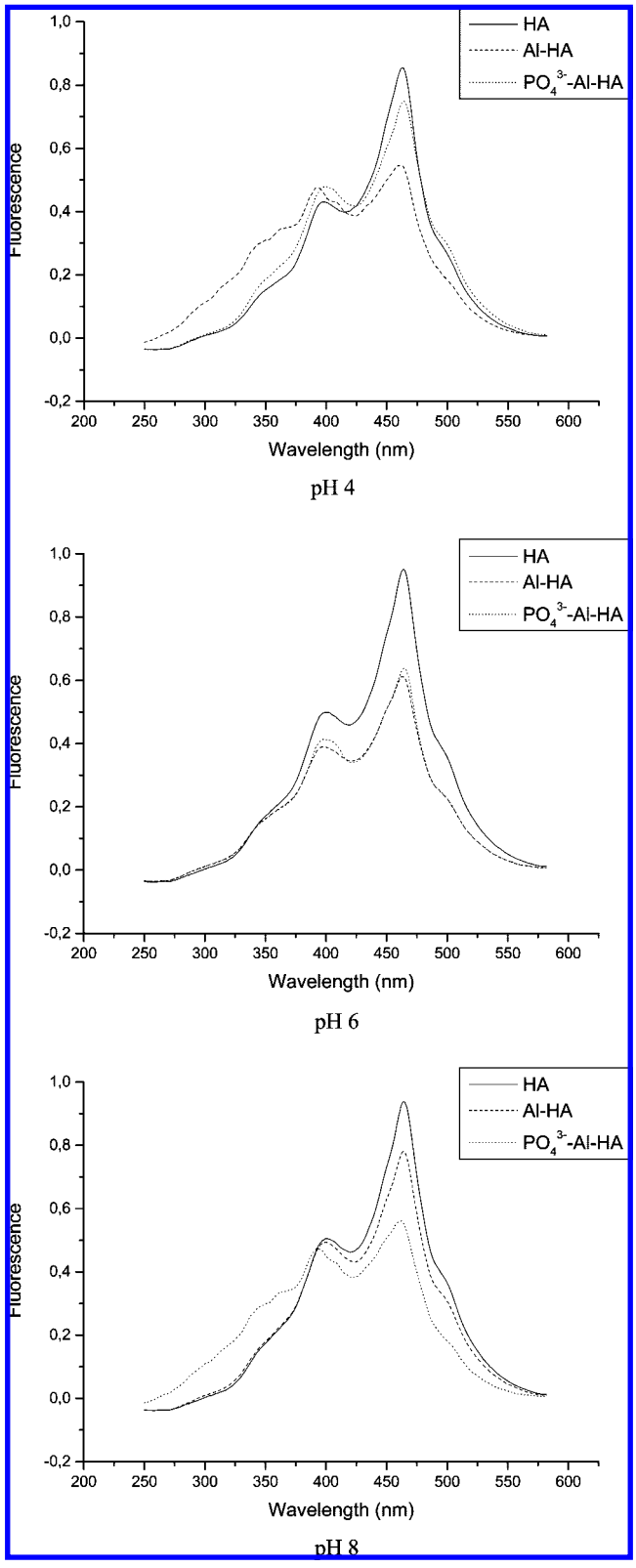

Figure 2. Synchronous fluorescence spectra ($\Delta\lambda$ = 18 nm) for HA, Al−HA complexes, and PO_4^{3-}−Al−HA complexes as a function of pH.

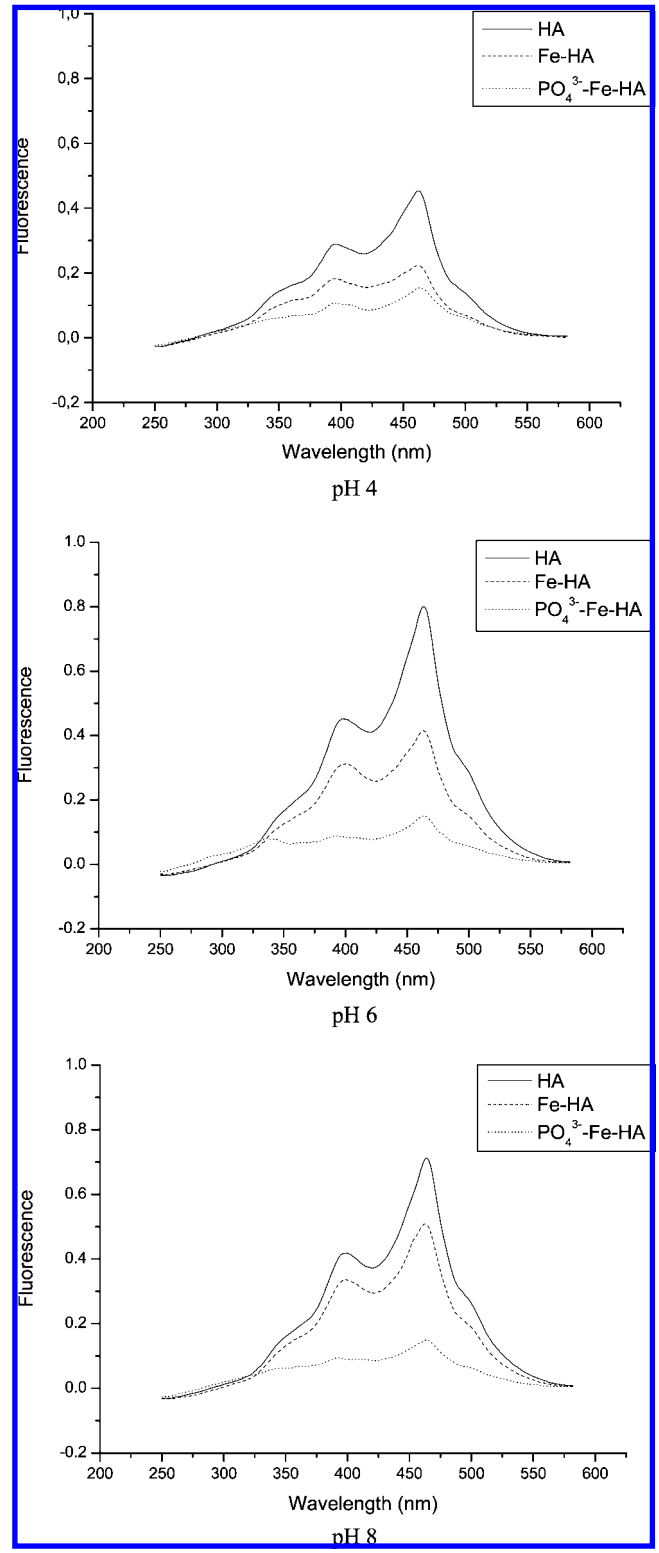

Figure 3. Synchronous fluorescence spectra ($\Delta\lambda$= 18 nm) for HA, Fe−HA complexes, and PO_4^{3-}−Fe−HA complexes as a function of pH.

pH, the interaction between the metal and phosphate seems to be more important than the M−HA interaction, whereas at alkaline pH the reverse is observed. In the case of Fe, however, a clear reinforcement of Fe−HA interaction could occur at all studied pH. These results were also concordant with the order of relative stability of the different M−HA complexes studied: Fe > Al > Zn (*6*). These results could also be associated, however, with the induction of steric effects that would affect the rigidity of the binding site and, consequently, fluorescence intensity (*16*).

The Molecular Modeling Study. To model the binding site present in HA for metal complexation we have selected a salicylic acid structural group (SA) with two ionization states: the ionization of the carboxylic group and the ionization of the carboxylic and phenolic groups.

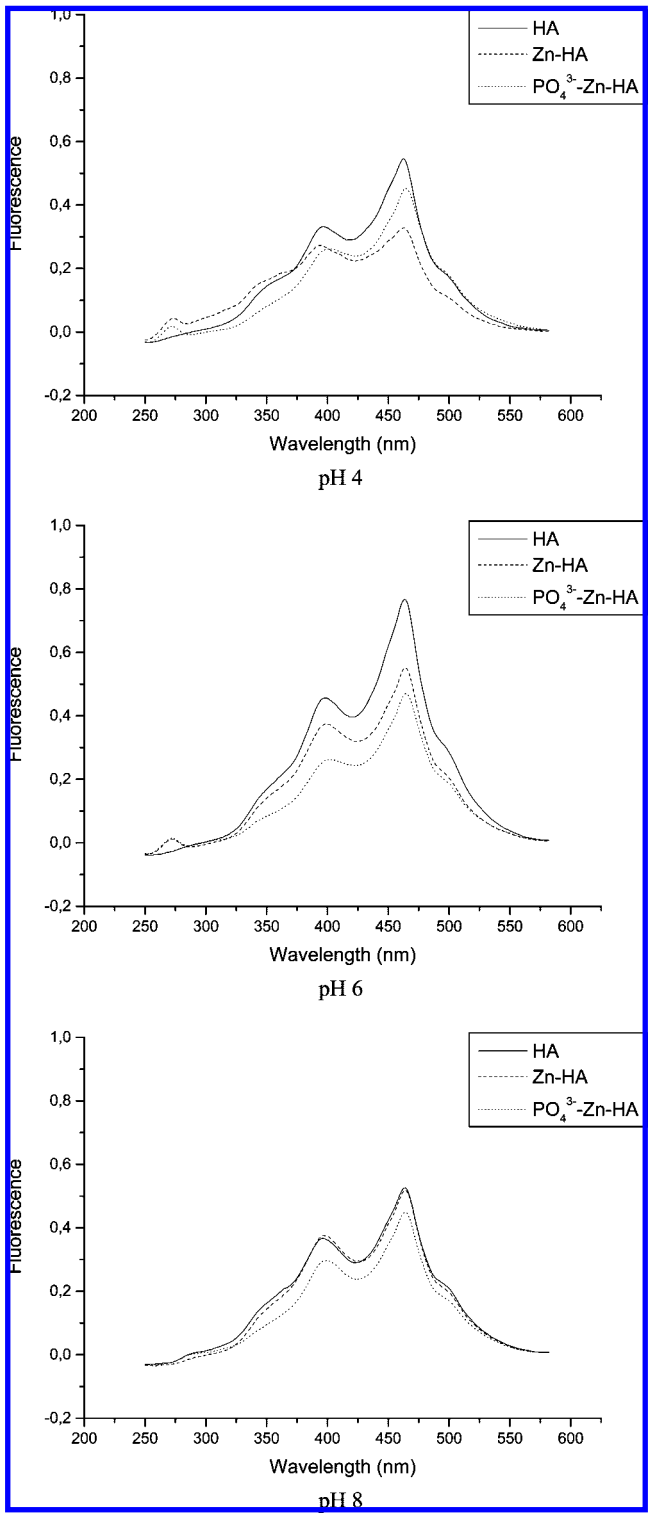

Figure 4. Synchronous fluorescence spectra ($\Delta\lambda$= 18 nm) for HA, Zn−HA complexes, and PO_4^{3-}−Zn−HA complexes as a function of pH.

For the Al−SA interaction in the case where only the ionization of the carboxylic group is considered SA^{-1}, the most stable intermolecular approaching interaction (electrostatic interaction) for Al complexation in SA, principally governed by electrostatic forces, is presented in Figure SI1 of the Supporting Information. This molecular configuration corresponds to the energy minimization of the molecular system using molecular mechanics (AMBER force field, structure $Al-SA^{-1}{}_{AMBER}$). As expected, it describes the interaction

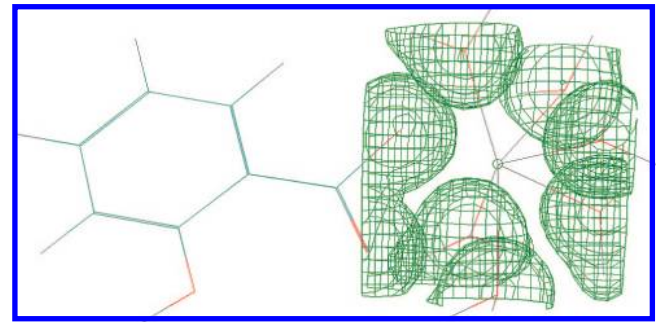

Figure 5. Binding interaction between the salicylic binding model (−1 charge) and Al. (The grid shaped globes represent the electronic density distribution for a contour value of 0.05 ea_0^{-3}.)

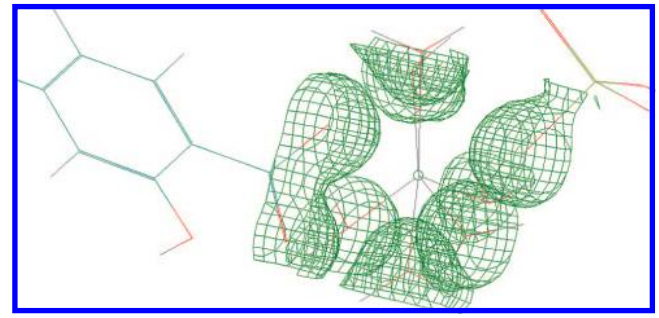

Figure 6. Binding interaction between $Al-SA^{-1}$ complex and phosphate. (The grid shaped globes represent the electronic density distribution for a contour value of 0.05 ea_0^{-3}.)

between the carboxylate and the metal in its hexahydrated form as well as some electrostatic interactions with the negative partial charges on the aromatic ring. To investigate the formation of more stable interactions (bonds with more covalent character, the binding interaction) we carried out an energy minimization of the system corresponding to $Al-SA^{-1}{}_{AMBER}$ using a semiempirical quantum chemical method (PM3). The molecular system obtained is presented in **Figure 5** (structure of $Al-SA^{-1}{}_{PM3}$). We also present the electronic density corresponding to Al (**Figure 5**). As can be observed, Al complexation in SA^{-1} involves the participation of the $C-O^-$ (bond distance 1.81 Å) and C—O (2.42 Å) in the carboxylate. Likewise, these interactions were associated with a significant enlargement of two Al−water bonds (from 1.88 to 2.41 and 2.46 Å). There is no participation of the phenol group in the binding process. The binding energy corresponding to this reaction was −343.38 kcal mol^{-1}. The distribution of the electronic density in the carboxylate suggests the presence of a bidentate pattern. This result was in line with the conclusions obtained from the FTIR study for Al−HA complexes (pH 4).

To investigate PO_4^{3-} binding in $Al-SA^{-1}$ we studied the electrostatic interaction and the binding interaction of the interaction of $Al-SA^{-1}{}_{PM3}$ with PO_4^{3-}. The most stable structure generated from the energy minimization of the molecular system $Al-SA^{-1}{}_{PM3}/PO_4^{3-}$ using AMBER is presented in Figure SI2 of the Supporting Information (structure: $Al-SA^{-1}-PO_4^{3-}{}_{AMBER}$). This structure involves the electrostatic interaction between the oxygen atoms of phosphate with the hydrogen atoms of the Al coordination water molecules. To calculate the binding interaction for $Al-SA^{-1}-PO_4^{3-}{}_{AMBER}$, we carried out an energy minimization of the system using PM3. This calculation generated the structure presented in **Figure 6** ($Al-SA^{-1}-PO_4^{3-}{}_{PM3}$; we also presented the electronic density on Al). The optimized structure describes the formation of a significant interaction between one oxygen

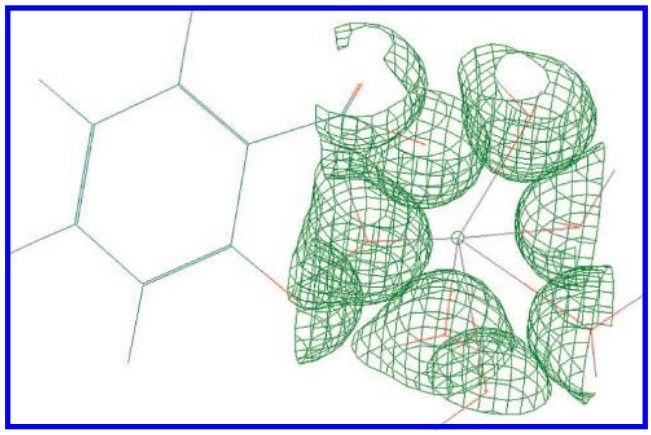

Figure 7. Binding interaction between the salicylic binding model (−2 charge) and Al. (The grid shaped globes represent the electronic density distribution for a contour value of 0.05 ea_0^{-3}.)

of PO_4^{3-} and Al (bond distance 1.8 Å), without any significant modification of the interaction between the SA carboxylate and Al. Likewise, AL−SA interaction presented a bidentate pattern in agreement with the FTIR study for Al−HA complexes (principally pH 6; it is important to note that we have not considered the possible formation of bidentate-bridging structures because we did not introduce two Al atoms in the calculation). These interactions were associated with a significant enlargement of Al−H_2O bond distances (between 2.43 and 2.46 Å). The binding energy corresponding to the reaction was −416.47 kcal mol^{-1}.

For the Al−SA interaction considering the ionization of both the carboxylic and phenolic groups (Al−SA^{-2}), the electrostatic interaction calculated using AMBER generated the most stable structure, presented in Figure SI3 of the Supporting Information (Al−$SA^{-2}{}_{AMBER}$). This structure describes the interaction of Al with both the carboxylate and the phenolate. The binding interaction corresponding to Al−$SA^{-2}{}_{AMBER}$ was calculated using PM3. This calculation generated the structure presented in **Figure 7** (Al−$SA^{-2}{}_{PM3}$), in which we include the electronic density on Al. As can be observed, this interaction involves the two oxygen atoms of the carboxylate (bond distances C−O−Al 1.86 Å, and C═O−Al 2.55 Å) and the oxygen of phenolate (bond distance 2.42 Å). This interaction was coupled to a significant enlargement of three Al−H_2O bonds (from 1.88 to 2.31, 2.38, and 2.41 Å). The distribution of electronic density in the carboxylate indicates a bidentate pattern, in agreement with the FTIR study for Al−HA complexes at pH 6. This result is also compatible with the binding pattern obtained from the FTIR study at pH 8 (bidentate-bridging) because we have not considered two metals in the calculation. The binding energy corresponding to the reaction was −605.7 kcal mol^{-1}.

As expected, Al complexation involving the ionization of both the carboxyl and phenol (ΔE_R = −605.7 kcal mol^{-1}) was significantly more stable than that only involving the ionization of the carboxyl (ΔE_R = −343.38 kcal mol^{-1}).

The more stable structure generated from the electrostatic interaction of Al−$SA(-2)_{PM3}$ with PO_4^{3-} is presented in **Figure SI4** of the Supporting Information (Al−SA^{-2}−$PO_4^{3-}{}_{AMBER}$). It includes the electrostatic interaction between two oxygen atoms of phosphate with the water coordination sphere of Al and with Al. The binding interaction study generated the structure presented in **Figure 8** (Al−SA^{-2}− $PO_4^{3-}{}_{PM3}$). It describes the interaction of one oxygen atom of phosphate with Al (bond distance 2.59 Å). There were not significant changes

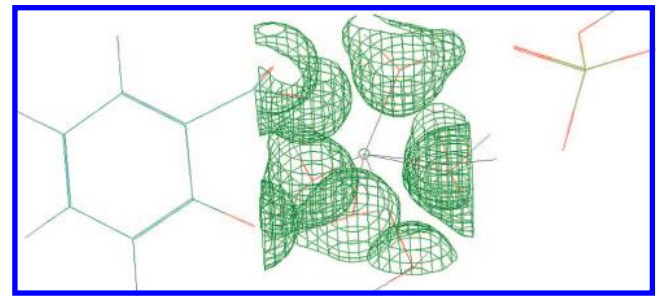

Figure 8. Binding interaction between Al−SA^{-2} complex and phosphate. (The grid shaped globes represent the electronic density distribution for a contour value of 0.05 ea_0^{-3}.)

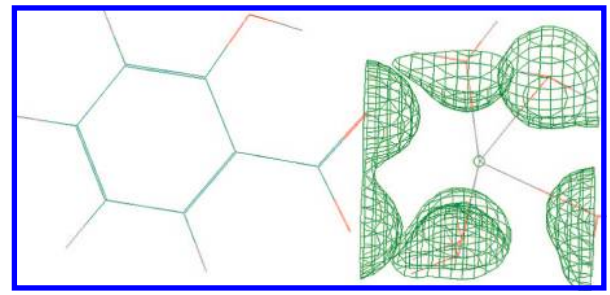

Figure 9. Binding interaction between the salicylic binding model (−1 charge) and Zn. (The grid shaped globes represent the electronic density distribution for a contour value of 0.05 ea_0^{-3}.)

in the electronic features of the Al−SA^{-2} interaction. The binding energy for this reaction was −287.49 kcal mol^{-1}.

It was noteworthy that the relative stability of the Al−SA^{-2}−PO_4^3 interaction was significantly less stable than that of the Al−SA^{-1}− PO_4^{3-} interaction. This result suggests that the stability of PO_4^{3-} fixation in Al−SA decreases in line with the increase in the stability of Al−SA complexes.

In the case of the interaction of SA with Zn(II), the structure generated by the electrostatic interaction study corresponding to the complexation of Zn in SA with only the carboxyl group ionized (SA(−1)) is presented in Figure SI5 of the Supporting Information (Zn−$SA^{-1}{}_{AMBER}$). As in the case of the Al−SA^{-1} interaction, it describes the interaction with the carboxylate and the negative partial charges on the aromatic ring. In **Figure 9**. we present the structure corresponding to the binding interaction study for Zn−$SA^{-1}{}_{AMBER}$ (Zn−$SA^{-1}{}_{PM3}$). This interaction involves the participation of the two oxygen atoms in the carboxylate (bond distances: C−O 2.13 Å and C−O 2.56 Å), with a slight enlargement of the Zn−H_2O bonds (from 2.14 to 2.17 to 2.29–2.26 Å). The electronic density distribution on the carboxylate suggests a bidentate pattern. In the FTIR study for Zn−HA at pH 4 (no ionization of phenol groups), the spectra indicated a bidentate-bridging model. These results may be compatible with our result because we have not considered several metal atoms in the calculation. The binding energy associated with this reaction was −204.25 kcal mol^{-1}.

The electrostatic interaction study corresponding to the interaction of Zn−$SA^{-1}{}_{PM3}$ with PO_4^{3-} generated the structure presented in Figure SI6 of the Supporting Information (Zn−SA^{-1}−$PO_4^{3-}{}_{AMBER}$). It describes an electrostatic interaction with the water coordination sphere and Zn atom. The binding interaction study for Zn−SA^{-1}−$PO_4^{3-}{}_{AMBER}$ generated the structure shown in **Figure 10** (Zn−SA^{-1}−$PO_4^{3-}{}_{PM3}$). This interaction involves the participation of two oxygen atoms of the phosphate group, one rather stable (bond distance 1.87 Å) and another less stable (bond distance 3.49 Å). This interaction significantly modified the bond distances of the interaction

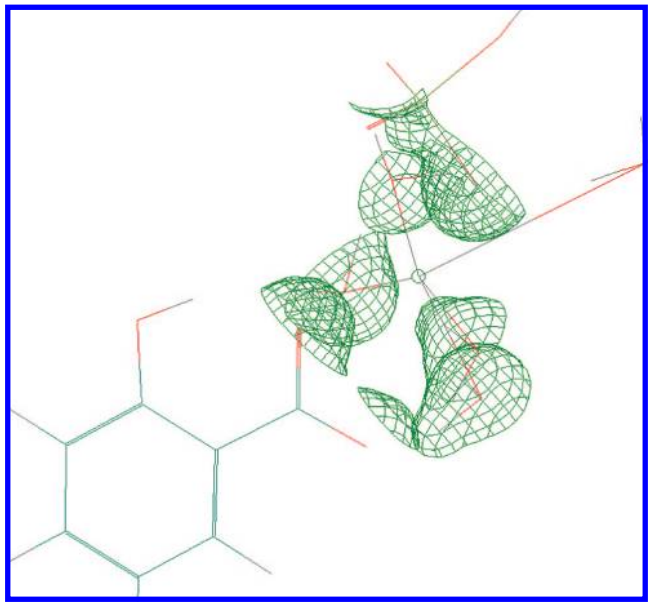

Figure 10. Binding interaction between $Zn-SA^{-1}$ complex and phosphate. (The grid shaped globes represent the electronic density distribution for a contour value of 0.05 ea_0^{-3}.)

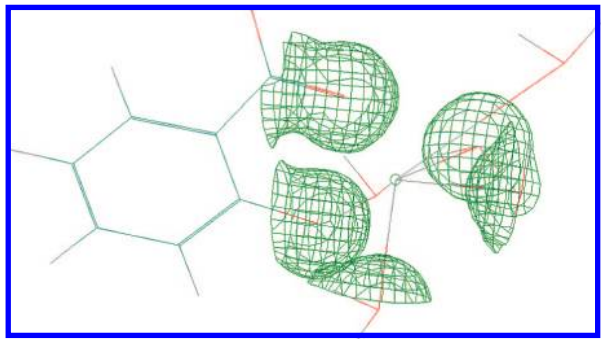

Figure 11. Binding interaction between the salicylic binding model (−2 charge) and phosphate. (The grid shaped globes represent the electronic density distribution for a contour value of 0.05 ea_0^{-3}.)

between the carboxylate with Zn. Thus, in the case of C═O a significant bond shortening was observed (from 2.56 to 2.16 Å), whereas for C—O a bond enlargement was noted (from 2.13 to 2.92 Å). These changes in bond distances indicate that a certain debilitation of the $Zn-SA^{-1}$ interaction, associated with PO_4^{3-} fixation, seems to occur. The electronic density distribution on the carboxylate indicated a possible bidentate pattern in agreement with the FTIR study for Zn−HA. On the other hand, one water molecule lost the interaction with Zn upon PO_4^{3-} fixation, and the other water molecules underwent significant bond enlargements. The binding energy for this reaction was −264 kcal mol^{-1}.

Regarding the interaction of Zn with SA and considering the ionization of both the carboxyl and phenolic groups, the electrostatic interaction study generated the structure presented in Figure SI7 of the Supporting Information ($Zn-SA^{-2}_{AMBER}$). It describes the interaction between the carboxylate and phenolate with the water coordination sphere of Zn and with Zn. The corresponding binding interaction study generated the structure presented in **Figure 11**. ($Zn-SA^{-2}_{PM3}$). This structure shows the involvement of the C═O of the carboxylate (bond distance 1.91 Å) and the O^- of phenolate (bond distance 1.95 Å). Two water molecules lost the interaction with Zn, and the other water molecules underwent a clear bond enlargement. The electronic density distribution on the carboxylate indicated a unidentate pattern in accordance with the FTIR study for Zn−HA at pH 6 and 8.

The binding energy for the reaction was −421.71 kcal mol^{-1}. As expected, the stability of the interaction involving the total ionization of the salicylate group ($\Delta E_R = -421.71$ kcal mol^{-1}) was more stable than that involving the ionization of the carboxylic group alone ($\Delta E_R = -204.25$ kcal mol^{-1}).

Concerning the study of PO_4^{3-} binding in $Zn-SA^{-2}_{PM3}$, the electrostatic interaction study did not generate any stable molecular configuration for the $Zn-SA^{-2}-PO_4^{3-}$ interaction. In consequence, PO_4^{3-} binding in Zn−SA is only theoretically expected for those Zn−SA complexes involving the ionization of only the carboxylate.

Regarding the possible application of the conclusions drawn from this study to the humic complexes, the fact that there was a reasonable concordance between the binding patterns for the carboxylate obtained from the FTIR study for PO_4^{3-}−M−HA complexes and those obtained from the theoretical study indicates that SA seems to be a good alternative to model the metal binding site in HA.

Thus, the results obtained for both the $Al-SA-PO_4^{3-}$ and the $Zn-SA-PO_4^{3-}$ interactions indicate that the stability, and even the formation, of PO_4^{3-}−M−SA (and possibly PO_4^{3-}−M−HA) complexes is conditioned by the stability of the M−SA(HA) complex: the more stable the metal complexes are, the less stable (and the possible formation) the phosphate complexes. This result could provide a possible explanation for the fact that only a relatively low fraction of complexed metal intervenes in phosphate fixation in M−HA (*6*). Only the metal fraction involved in HA complexes with low stability will be able to form stable phosphate complexes. The theoretical study indicates that this situation might be related to the metal fraction complexed with only one carboxylate. Thus, the results obtained suggest that, in the case of $Zn-HA-PO_4^{3-}$ complexes, only the fraction of Zn complexed by a carboxylic group participates in phosphate binding. This would also be the case for the more stable fraction of $Al-HA-PO_4^{3-}$. This carboxylate may be integrated in a more complex binding site (such as the salicylic structure) or, more probably, may correspond to isolated groups. This result also provides a complementary explanation for the relatively low fraction of complexed metal that is involved in the formation of stable PO_4^{3-}−M−HA complexes (*4, 6*), because several studies indicate that the majority of carboxylic groups are probably grouped with other carboxylates (phthalate type structure) or with phenols (salicylate type structure). So, the relative concentration of isolated carboxylic groups in HA is expected to be rather low.

Regarding the relative stability of phosphate complexes involving Al and Zn, the results obtained indicate that $Al-SA-PO_4^{3-}$ complexes presented more stability than $Zn-SA-PO_4^{3-}$. This result is in line with those obtained concerning the apparent stability of PO_4^{3-}−M−HA complexes involving Al and Zn (*6*). They also indicate that Al−SA complexes are more stable than Zn−SA complexes. This result is concordant with the relative stability of Al−HA and Zn−HA complexes (*11, 16*).

In summary, the FTIR study indicated that, in the case of those complexes involving Fe and Zn phosphate, fixation is associated with a stabilization of the metal−carboxylate bond. In the case of Al, this effect is less clear. This effect of phosphate fixation on the characteristics of the metal−humic binding site was also supported by the results obtained in the fluorescence study, which showed significant changes in the quenching effect,

normally associated with metal complexation in humic substances, upon phosphate fixation.

Finally, the molecular modeling study revealed that the stability of PO_4^{3-}−M−humic complexes is inversely related to the stability of metal−humic interaction. This result could explain why only a relatively low proportion of humic complexed metal is involved in phosphate fixation.

ABBREVIATIONS USED

M, metal; PO_4^{3-}, phosphate; SA, salicylic acid; HA, humic acid.

This research was funded by the Roullier Group and the Government of Navarra.

ACKNOWLEDGMENT

Special thanks to David Rhymes for improving the English of the article.

Supporting Information Available: Figures SI1−7 present the electrostatic interaction between the SA model and Al or Zn. This material is available free of charge via the Internet at http://pubs.acs.org.

LITERATURE CITED

(1) Broadbent, F. E. Effects of organic matter on nitrogen and phosphorus supply to plants. In *The Role of Organic Matter in Modern Agriculture*; Chen, Y., Avnimelech, Y., Eds.; Martinus Nijhoff Publishers: Dordrecht, The Netherlands, 1986; pp 13–27.

(2) Chen, Y.; De Nobili, M.; Aviad, T. Stimulatory effects of humic substances on plant growth. In *Soil Organic Matter in Sustainable Agriculture*; Magdoff, F., Weil, R. R., Eds.; CRC Press: Boca Raton, Florida, 2004; pp 103–129.

(3) Delgado, A.; Madrid, A.; Kassem, S.; Andreu, L.; Del Campillo, M. C. Phosphorus fertilizer recovery from calcareous soils amended with humic and fulvic acids. *Plant Soil* **2002**, *245*, 277–286.

(4) Guardado, I.; Urrutia, O.; García-Mina, J. M. Methodological approach to the study of the formation and physicochemical properties of phosphate−metal−humic complexes in solution. *J. Agric. Food Chem.* **2005**, *53*, 8673–8678.

(5) Riggle, J.; von Wandruszka, R. Binding of inorganic phosphate to dissolved metal humates. *Talanta* **2005**, *66*, 372–375.

(6) Guardado, I.; Urrutia, O.; García-Mina, J. M. Size distribution, complexing capacity and stability of phosphate−metal−humic complexes. *J. Agric. Food Chem.* **2007**, *55*, 408–413.

(7) Takamatsu, T.; Yoshida, T. Determination of stability constants of metal−humic acid complexes by potentiometric titration and ion-selective electrodes. *Soil Science* **1978**, *125*, 377–386.

(8) Allinger, N. Conformational analysis 130 MM2. A hydrocarbon force field utilizing V1 and V2 torsional terms. *J. Am. Chem. Soc.* **1977**, *99*, 8127–8134.

(9) Weiner, S. J.; Kollman, P. A.; Case, D. A.; Singh, U. C.; Ghio, C.; Alagona, G.; Profeta, S.; Weiner, P. A new force field for molecular mechanics simulation of nucleic acids and proteins. *J. Am. Chem. Soc.* **1984**, *106*, 765–784.

(10) Stewart, J. J. Optimization of parameters for semiempirical methods I. Method. *J. Comput. Chem.* **1989**, *10*, 209–220.

(11) Stevenson, F. J. *Humus Chemistry*, 2nd ed.; Wiley: New York, 1994.

(12) Garcia-Mina, J. M. Stability, solubility and maximum metal binding capacity in metal-humic complexes involving humic substances extracted from peat and organic compost. *Org. Geochem.* **2006**, *37*, 1960–1972.

(13) Cotton, A. F.; Wilkinson, G. *Advanced Inorganic Chemistry*; Wiley-Interscience: New York, 1986.

(14) Nakamoto, K. *Infrared and Raman Spectra of Inorganic and Coordination Compounds*; Wiley-Interscience, New York; 1978.

(15) Baigorri, R.; García-Mina, J. M.; González-Gaitano, G. Supramolecular association induced by Fe(III) in low molecular weight sodium polyacrylate. *Colloids Surf. A* **2007**, *292*, 212–216.

(16) Senesi, N. Metal−humic substance complexes in the environment. Molecular and mechanistic aspects by multiple spectroscopic approach. In *Biogeochemistry of Trace Metals*; Lewis Publishers: New York, 1992; pp 429–496.

Received for review September 6, 2007. Revised manuscript received November 18, 2007. Accepted November 21, 2007.

JF072641K